Solid State Ionics 324 (2018) 109–113

Contents lists available at ScienceDirect

Solid State Ionics

journal homepage: www.elsevier.com/locate/ssi

Ternary $LiBH_4$-$NaBH_4$-MgH_2 composite as fast ionic conductor

Mengyuan Xiang[a], Yao Zhang[a,c,*], Yunfeng Zhu[b,c,*], Xinli Guo[a], Jian Chen[a], Liquan Li[b,c]

[a] School of Materials Science and Engineering, Jiangsu Key Laboratory of Advanced Metallic Materials, Southeast University, Nanjing 211189, China
[b] College of Materials Science and Engineering, Nanjing Tech University, 5 Xinmofan Road, Nanjing 210009, China
[c] Jiangsu Collaborative Innovation Center for Advanced Inorganic Function Composites, Nanjing Tech University, Nanjing 210009, China

ARTICLE INFO

Keywords:
Ionic conductivity
Electrochemical stability
Ionic mobility
$LiBH_4$-$NaBH_4$-MgH_2 composite

ABSTRACT

In the present paper, ball milled $LiBH_4$-$NaBH_4$-MgH_2 ternary-phase composite achieves nearly 100 times as much as the lithium ionic conductivity of the pristine $LiBH_4$ at a temperature below 373 K. $4LiBH_4$-$NaBH_4$-30%MgH_2 possesses ionic conductivity of 11.2 ms cm^{-1} at a temperature of 383 K, which is almost 100 times higher than that of pristine $LiBH_4$. Furthermore, cyclic voltammetry (CV) measurements on these composite samples identified a wide potential window ranging from −1 V to 4 V, demonstrating the electrochemical stability of these samples when Li^+ ions has been transported. Both X-ray diffraction (XRD) and Fourier Transform infrared spectroscopy (FTIR) results verified the structural stability of $LiBH_4$-$NaBH_4$-MgH_2 composites during the temperature ramping process. Both phase transformation enthalpies and temperatures for $LiBH_4$ were all reduced according to differential scanning calorimetry (DSC) measurements, implying that the high temperature phase of $LiBH_4$ could be effectively stabilized by co-additives of $NaBH_4$-MgH_2.

1. Introduction

As well known, liquid electrolytes easily lead to the formation of dendrites and raise the hazards of short circuit or burning [1–4]. For these reasons, solid electrolytes or all solid state batteries [1, 2] have been extensively investigated. Comparing with liquid electrolytes, solid electrolyte exhibits many advantages e.g. reduced weight and volume, improved energy output, and inhibited lithium dendrites [1–4]. Therefore, solid lithium ion conductors attract much interest from all over the world in recent decades [5–10]. Up to date, such solid electrolytes as LISICON-type [11], NASICON-type [12], garnet-type [13–16] and perovskite [17–21] or anti perovskite-type [22] etc. have been intensively studied. Unfortunately, lithium ionic conductivities of most solid electrolytes still hardly approach to the level of liquid ones at a room temperature [23, 24].

Among those solid electrolytes, $LiBH_4$ have attracted much attention over past ten years due to its high conductivity at a temperature above 383 K [25, 26]. It usually undergoes a structural transition from orthorhombic phase to hexagonal phase at around 383 K. The conductivity could attain 10^{-2} S cm^{-1} at above 383 K [27] while it would be decreased to 10^{-8} S cm^{-1} at room temperature. Therefore, stabilization of the HT phase at low temperature is highly desired. Furthermore, ionic conductivities of $LiBH_4$-$NaBH_4$ system and $LiBH_4$-MgH_2 [25] system are greatly improved from that of pristine $LiBH_4$ [28] according to our previous studies. Both chemical and electrochemical stabilities were enhanced as well. Therefore, in $LiBH_4$-$NaBH_4$-MgH_2 ternary composite, we also expect that MgH_2 and $NaBH_4$ might synergistically enhance the ionic conductivity of samples. The defects at the grain boundaries would be available to increase the grain boundary conductivity [29].

In the present work, the ionic conductivity of $LiBH_4$-$NaBH_4$-MgH_2 ternary composites is higher than that of pristine $LiBH_4$. Similarly, their phase structures were investigated by means of X-ray diffraction (XRD), Fourier transform infrared spectra and Raman spectra. Their thermal stability was studied by diffraction scanning calorimetry (DSC). We examined the electrochemical stability of $LiBH_4$-$NaBH_4$-MgH_2 composites by means of cyclic voltammetry (CV).

2. Experimental section

2.1. Preparation of the $LiBH_4$-$NaBH_4$-MgH_2 composites

$NaBH_4$-MgH_2-added $LiBH_4$ were synthesized by means of conventional solid-state reaction method. These raw materials were mixed in a pot of a planetary ball mill (QM-1SP) and ball-milled for 20 h at a rotation rate of 450 rpm. All measurements were implemented in a glove box which is full of argon. Both oxygen and water densities are all lower than 0.1 ppm.

* Corresponding authors at: Jiangsu Collaborative Innovation Center for Advanced Inorganic Function Composites, Nanjing Tech University, Nanjing 210009, China.
E-mail addresses: zhangyao@seu.edu.cn (Y. Zhang), yfzhu@njtech.edu.cn (Y. Zhu).

https://doi.org/10.1016/j.ssi.2018.06.015
Received 3 May 2018; Received in revised form 8 June 2018; Accepted 18 June 2018

2.2. Structural characterization

The crystal structures of samples with different amount of MgH_2 were characterized by X-Ray diffraction (XRD, SmartLab TM 3 kW diffractometer) using Cu Kα radiation with a 2θ range of 20–80°. Each sample pool was covered by an amorphous polymer film (Scotch 810# Magic Tape) for escaping air and humidity. The Fourier transform infrared spectrometer (FTIR, Thermo Nicolet 5700) were used to observe the internal groups of each samples. And the wavenumber ranges from 4000 cm^{-1} to 500 cm^{-1}.

2.3. Ionic conductivity

Sample's powders were pressed into pellets with a diameter of 12.5 mm under a pressure of 20 MPa. They were covered by two lithium foils (Lizhiyuan, 99%) on both sides to form test electrodes, and loaded in an airtight sample holder. Ionic conductivity of $LiBH_4$-$NaBH_4$-xMgH_2 (x = 10%, 20%, 30%) composites were examined within a temperature range from 303 K to 393 K by alternating current (AC) impedance spectroscopy (a CHI660e electrochemical workstation, Shanghai Chenhua Co. Ltd) with a frequency range of 1 MHz to 1 Hz and an applied amplitude of 0.02.

2.4. Cyclic voltammetry (CV)

Cyclic voltammetry (CV) measurements on $LiBH_4$-$NaBH_4$-MgH_2 were examined on the same electrochemical workstation as impedance measurements. A lithium foil covered the pellets as previous work [16, 17]. Their structure can be described as $LiBH_4$-$NaBH_4$-MgH_2|Li. The lithium foil is reference electrode. The scanning rate was 10 mV s^{-1} from −1 V to 3 V.

2.5. Differential scanning calorimetry (DSC)

DSC measurements were conducted upon a TA Q2000 instrument at a ramping rate of 2 K min^{-1}. Approximately 2 mg sample powder was loaded in each pan. High-purity Ar (99.9999%, 0.1 MPa) was employed as purging gas, of which the flow rate was 20 mL min^{-1}.

3. Results

3.1. Phases' structures

Fig. 1 shows XRD patterns of $LiBH_4$-$NaBH_4$-MgH_2 composites after ball milling. These patterns indicate that both MgH_2 and $NaBH_4$ phases were perfectly maintained in all $LiBH_4$-$NaBH_4$–xMgH_2 samples (x = 10%, 20%, 30%, respectively). The absence of $LiBH_4$ diffraction peaks might be attributed to the amorphous phase as mentioned in previous work [30]. The crystallites sizes of both $NaBH_4$ and MgH_2 phases could be identified by Scherrer's equation [31, 32].

$$D = K\gamma/B\cos\theta \quad (1)$$

In this equation, D reflects the average crystallite size (nm); K represents the Scherrer constant; γ is the wavelength of X-ray, a constant of 0.154056 nm. B is the FWHM of diffraction peaks of the samples. θ is the Bragg angle.

$NaBH_4$ and MgH_2 phases can be observed in XRD pattern of Fig. 1. $LiBH_4$ phase cannot be characterized due to its amorphous state. However, FTIR spectra in Fig. 2 and Raman spectra in Fig. 3 strongly demonstrated the presence of B—H bands belonging to $LiBH_4$ in ball milled $LiBH_4$-$NaBH_4$-MgH_2 composite. In addition, the stretching vibration (γ_1) of the $NaBH_4$ in as-milled $LiBH_4$-$NaBH_4$-MgH_2 (x = 10%, 20%, 30%, respectively) mixture was identified as 2323 cm^{-1}, which is lower than that of as-milled $NaBH_4$ (2331 cm^{-1}) [33].

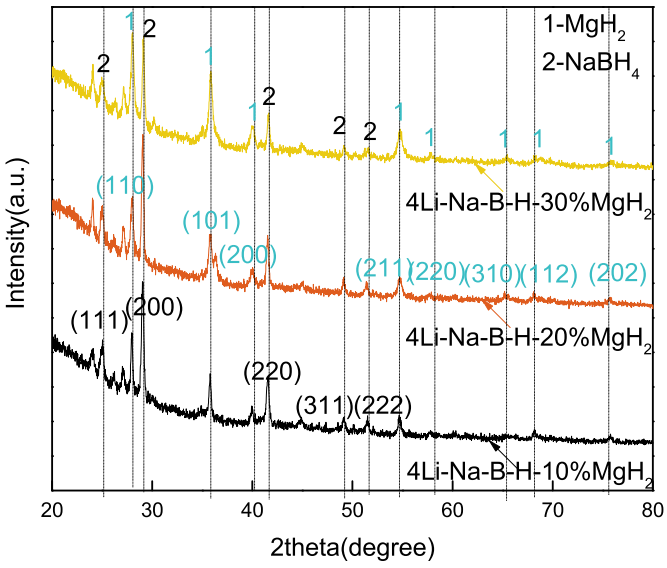

Fig. 1. XRD patterns of $LiBH_4$-$NaBH_4$–MgH_2 samples after ball milling.

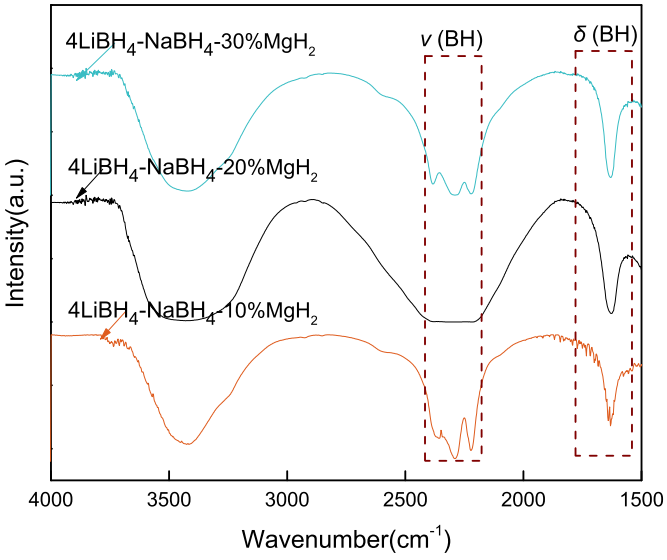

Fig. 2. FTIR spectra of $LiBH_4$-$NaBH_4$–MgH_2 samples after ball milling.

3.2. Conductivity

Nyquist diagrams of $LiBH_4$-$NaBH_4$-MgH_2 composite tested at different temperatures were displayed in Supplementary Figs. 1–3.

These semicircles are well fitted by the equivalent circuit of the Nyquist plot (the 4th diagram in Supplementary Figs. 1–3) in which the resistance R and the constant-phase element CPE are parallel components. This circuit yields a fitting deviation of 0.04, which is the lowest value among those models summarized in Table 1. The charge transfer resistance R in the following formula is defined by the intersection of the semicircle in the low frequency limit and the Z real axis related to the ionic conductivity σ of the electrolyte [34].

$$\sigma = \frac{d}{AR} \quad (2)$$

In which A reflects the area of the pellet surface and d represents the thickness of these sample. The calculated σ values were exhibited in Fig. 4 where temperature dependencies of ionic conductivity for different $LiBH_4$-$NaBH_4$–xMgH_2 samples (x = 10%, 20%, 30%, respectively) as well as pristine $LiBH_4$ were plotted by Arrhenius equation.